How to cite: *Angew. Chem. Int. Ed.* **2024**, *63*, e202317416
doi.org/10.1002/anie.202317416

Silicon Chemistry

Stabilization of NH– Group Adjacent to Naked Silicon(II) Atom in Base Stabilized Aminosilylenes

Madhusudan K. Pandey, Zohreh Hendi, Xiaobai Wang, Anirban Bhandari, Mukesh K. Singh, Katharina Rachuy, Saroj Kumar Kushvaha, Regine Herbst-Irmer, Dietmar Stalke,* and Herbert W. Roesky**

Dedicated to Professor Maravanji S. Balakrishna on the occasion of his 64th birthday

Abstract: Aminosilylene, comprising reactive NH– and Si(II) sites next to each other, is an intriguing class of compounds due to its ability to show diverse reactivity. However, stabilizing the reactive NH– group next to the free Si(II) atom is challenging and has not yet been achieved. Herein, we report the first examples of base stabilized free aminosilylenes Ar*NHSi(PhC(N^{t}Bu)$_2$) (**1a**) and Mes*NHSi(PhC(N^{t}Bu)$_2$) (**1b**) (Ar* = 2,6-dibenzhydryl-4-methylphenyl and Mes* = 2,4,6-tri-tert-butylphenyl), tolerating a NH– group next to the naked Si(II) atom. Remarkably, **1a** and **1b** exhibited interesting differences in their reactivity upon heating. With **1a**, an intramolecular C(sp^3)–H activation of one of the benzhydryl methine hydrogen atoms to the Si(II) atom produced the five-membered cyclic silazane **2**. However, with **1b**, a rare 1,2-hydrogen shift to the Si(II) atom afforded a silanimine **3**, with a hydride ligand attached to an unsaturated silicon atom. Further, the coordination capabilities of **1a** were also tested with Ru(II) and Fe(0) precursors. Treatments of **1a** with [Ru(η^6-*p*-cymene)Cl$_2$]$_2$ led to the isolation of a η^6-arene tethered complex [RuCl$_2$\{Ar*NHSi(PhC(^{t}BuN)$_2$)-κ^1-*Si*-η^6-arene\}] (**4**), whereas with the Fe(CO)$_5$ precursor a Fe(0) complex [Fe(CO)$_4$\{Ar*NHSi(PhC(^{t}BuN)$_2$)-κ^1-*Si*\}] (**5**) was obtained. Density functional theory (DFT) calculations were conducted to shed light on the structural, bonding, and energetic aspects in **1**–**5**.

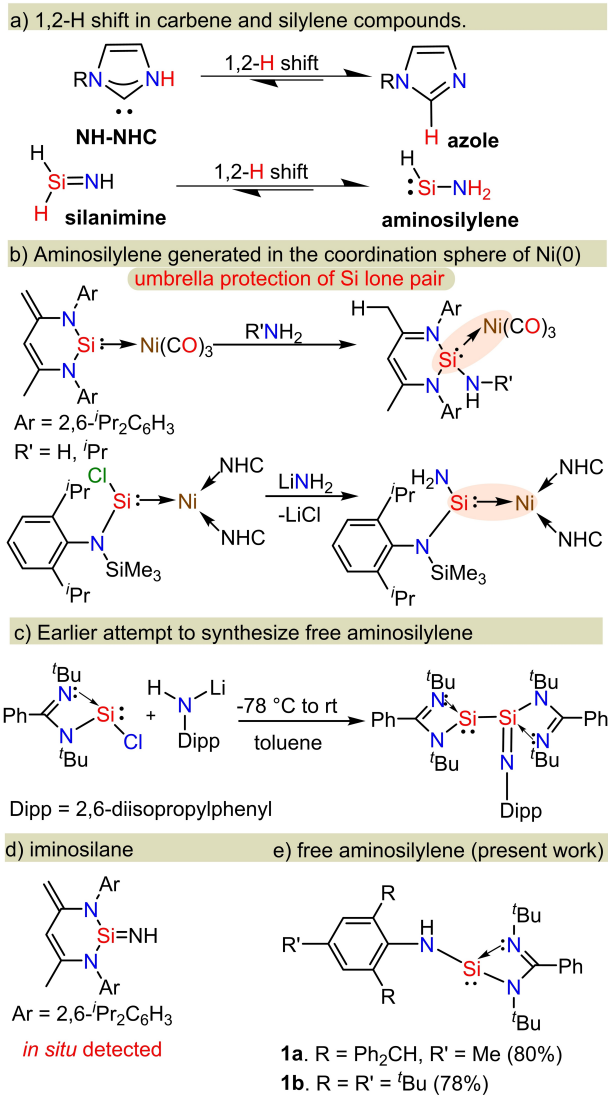
Introduction

The compounds of Group-14 low-valent elements have drawn significant interest in the recent past owing to their unique reactivity, catalytic activities, and abilities to stabilize metals in unusual oxidation states.[1–7] Highly reactive compounds of low-valent elements of Group-14 have been obtained and structurally characterized using the concept of kinetic and/or thermodynamic stabilization.[8–12] However, stabilizing reactive groups such as NH–, OH–, and SH– next to highly nucleophilic free carbene and silylene centres is very challenging because of its tendency to tautomerize or react with itself intra- or intermolecularly to give undesired compounds.[13–16] In the realm of N-heterocyclic carbene (NHC) chemistry, the replacement of one of the NR groups from the traditional NR, NR-NHCs by NH– led to the development of protic N-heterocyclic carbenes (*p*NHC). However, the isolation of free *p*NHC is eluded to date, mainly because the NH– group next to the nucleophilic carbene carbon atom renders the free NH-NHC form less stable than the corresponding azole form (Scheme 1a).[17–18] Macgregor et al. opined that the NH-NHC form of the *p*NHC can be stabilized if the sterically demanding group is placed near the NH– residue.[19] Contrary to this, the aminosilylene form (HSi–NH$_2$) is more stable than silanimine (H$_2$Si=NH) by 70 kJ/mol^{-1} in silylene chemistry (Scheme 1a).[20] In 1994, West and Denk reported the first example of stable two-coordinate silylene 1,3-di-*tert*-2,3-dihydro-1*H*-1,3,2-diazasilol-2-ylidene.[21] This discovery encouraged researchers to synthesize several stable silylenes and further explore their chemistry.[22–23] However, it was not until 2006[24] that Roesky and co-workers isolated the first

[*] Dr. M. K. Pandey, Dr. Z. Hendi, X. Wang, K. Rachuy, Dr. S. Kumar Kushvaha, Dr. R. Herbst-Irmer, Prof. Dr. D. Stalke, Prof. Dr. H. W. Roesky
Institut für Anorganische Chemie, Georg-August-Universität Göttingen
37077 Göttingen (Germany)
E-mail: dstalke@chemie.uni-goettingen.de
hroesky@gwdg.de
Dr. A. Bhandari
Department of Chemistry, Seoul National University
1 Gwanak-ro, Gwanak-gu, Seoul 08826 (Republic of Korea)
Dr. M. K. Singh
School of Chemistry, University of Edinburgh
EH93FJ Edinburgh (UK)
E-mail: msingh2@ed.ac.uk

© 2023 The Authors. Angewandte Chemie International Edition published by Wiley-VCH GmbH. This is an open access article under the terms of the Creative Commons Attribution License, which permits use, distribution and reproduction in any medium, provided the original work is properly cited.

© 2023 The Authors. Angewandte Chemie International Edition published by Wiley-VCH GmbH



Scheme 1. a) 1,2-Hydrogen shift in carbene and silylene compound is demonstrated. b) Aminosilylene generated in the coordination sphere of Ni(0). c) Earlier attempts to synthesize free aminosilylene resulted in an unusual silaiminyl-silylene Si(I)–Si(III) compound. d) iminosilane (in situ detected). e) Free aminosilylenes (This work).

example of heteroleptic chlorosilylene stabilized by amidinate ligand.[25] The facile synthesis of chlorosilylene, with an easily functionalizable Si–Cl bond,[26] resulted in easy access to a plethora of Si(II) systems.[27–28] Silylenes are better σ-donor than phosphines and carbenes.[29] As a result, several functionalized silylenes have been synthesized and utilized to isolate several low-valent main group elements in low-valent oxidation states.[30–32] Furthermore, metal complexes stabilized with functionalized silylenes have proven to be effective catalysts in various challenging transformations.[33] However, to the best of our knowledge, the aminosilylene class of compounds, where the reactive NH– group is present next to the naked Si(II) atom, is unknown. Aminosilylene ($HSi–NH_2$) is only observed experimentally in the gas phase.[20] Driess and co-workers, in their elegant work, utilized an umbrella protection strategy to isolate the aminosilylene in the coordination sphere of the Ni(0).[15,34] They could isolate the aminosilylene, when the lone pair of silylene is coordinated to a Ni(0) atom (Scheme 1b). In their approach to synthesize the aminosilylene class of compounds, P. Roesky et al. attempted the reaction of mono-lithiated amide [DippN(H)Li] (Dipp = 2,6-diisopropylphenyl) with heteroleptic chlorosilylene [(PhC-(^{t}BuN)$_2$SiCl], which resulted in the formation of an unusual Si(I)–Si(III) mixed valent compound (Scheme 1c).

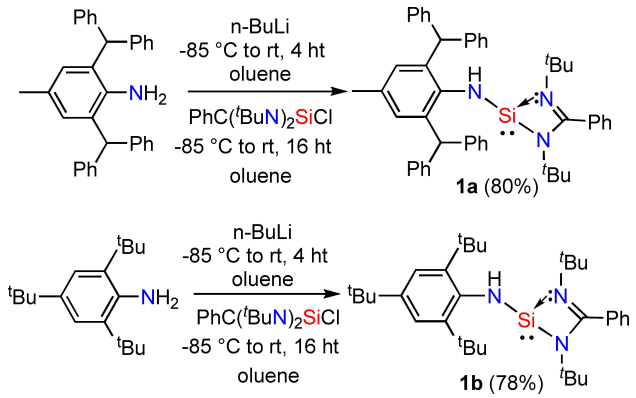
It was suggested that the reaction proceeds via the formation of aminosilylene as an intermediate.[16] Driess and co-workers could detect the *"half-parent"* aminosilylene, a highly reactive ylidic imino-silane compound, in situ during the reaction (Scheme 1d).[35] To the best of our knowledge, there is no report on the synthesis and isolation of the aminosilylene class of challenging compounds in its free form. Our interest in synthesizing aminosilylene class of challenging compounds stems from their multifaceted behavior in main-group chemistry, where the NH– group can be deprotonated both (before and after complexation) to afford several interesting low-valent main-group compounds. This class of compounds can also show metal-ligand cooperation during catalytic reactions,[36] a well-known phenomenon with phosphines and carbenes that has not yet been explored in silylene chemistry. With this in mind, we utilized the concept of steric protection of the NH– group to synthesize aminosilylenes **1a** and **1b** in their free form. The DFT calculation showed that the orientation of the NH– group and Si(II) lone pair is *trans* in bulky aminosilylenes. Hence, it needs prior reorganization to come to the same plane for the 1,2-hydrogen shift (see below). Additionally, the bulky groups might also help prevent undesired intermolecular reactions. Herein, we report the synthesis, reactivity, and coordination capabilities of this novel class of compounds.

Results and Discussion

The investigation was started with sterically demanding anilines (2,6-dibenzhydryl-4-methylaniline and 2,4,6-tri-tert-butylaniline), hoping that bulky side arms might help in stabilizing the reactive NH– group next to naked Si(II) atom. Indeed, a 1:1 salt metathesis reaction of lithiated amides [Li{NH(Ar*/Mes*)}], generated in situ with heteroleptic chlorosilylene [(PhC(N^{t}Bu)$_2$SiCl][26] resulted in the formation of aminosilylenes Ar*NHSi(PhC(N^{t}Bu)$_2$) (**1a**) and Mes*NHSi(PhC(N^{t}Bu)$_2$) (**1b**), respectively in good yield as off-white solids (Scheme 2). The presence of the NH– group adjacent to the naked Si(II) atom is the feature of **1a** and **1b** that distinguishes them from the previously reported amidinato-silylenes.[37] Both compounds **1a** and **1b** are stable in the solid state and under a toluene solution at room temperature for months, and no detectable tautomerization or decomposition was observed. The presence of bulky side-arms groups, which shield the Si(II) atom in the ligand backbone, might be the reason for this remarkable stability.

© 2023 The Authors. Angewandte Chemie International Edition published by Wiley-VCH GmbH

15213773, 2024, 9, Downloaded from https://onlinelibrary.wiley.com/doi/10.1002/anie.202317416, Wiley Online Library on [07/11/2026]. See the Terms and Conditions (https://onlinelibrary.wiley.com/terms-and-conditions) on Wiley Online Library for rules of use; OA articles are governed by the applicable Creative Commons License



Scheme 2. Synthesis of **1a** and **1b**.

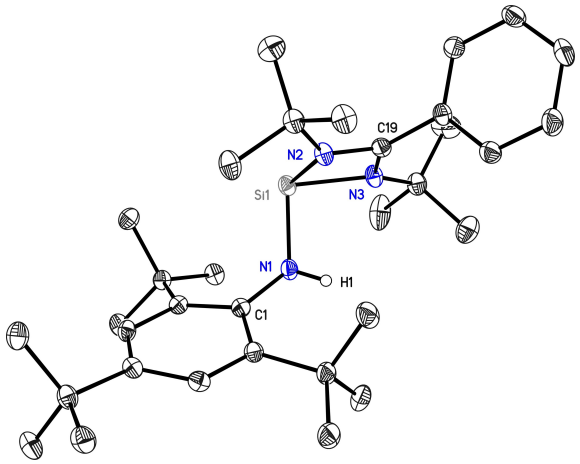
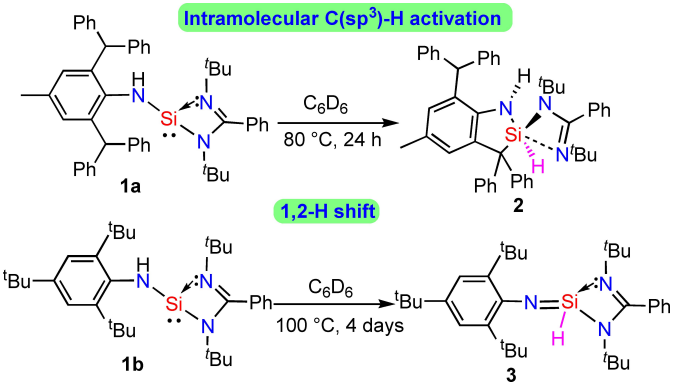


Figure 1. Molecular structure of **1b**. The anisotropic displacement parameters are depicted at the 50% probability level. Hydrogen atoms, except NH–, have been omitted for clarity. Selected bond lengths (Å) and bond angles (°). N1–Si1 1.7935(10), N2–Si1 1.9024(10), N3–Si1 1.8781(10), C1–N1 1.4095(13), N1–Si1–N2 102.65(4), N1–Si1–N3 95.11(5).

Both aminosilylenes **1a** and **1b** are well-characterized by nuclear magnetic resonance (NMR) and infrared (IR) spectroscopies, liquid injection field desorption ionization (LIFDI) mass spectrometry, and elemental analysis. (see Supporting Information: Figures S1–S19). The $^{29}Si\{^{1}H\}$ and ^{29}Si NMR spectra of **1a** and **1b** showed a singlet resonance at −3.4 and −4.0 ppm, respectively, which is similar to the same for R_2NSi(amidinate) (R = Cy, ^{i}Pr).[37] The ^{1}H NMR spectra of **1a** and **1b** showed singlets at 0.91 and 1.06 ppm for N^{t}Bu protons, respectively. In contrast, the characteristic NH– proton exhibited a singlet at 4.21 and 4.93 ppm, respectively. The aromatic protons appeared in the range of 6.89–7.49 ppm. The LIFDI mass spectrum of **1a** and **1b** showed molecular ions for $[M]^+$ at 697.4 (m/z = 697.3852) and 519.9 (m/z = 519.4009), respectively, confirming the desired compound formation (see Supporting Information: Figures S9 and S18). Single crystals of **1b** suitable for X-ray diffraction analysis were grown from a saturated toluene solution of **1b** at room temperature over one month. Compound **1b** crystallizes in the monoclinic space group $P2_1/n$ (see Supporting Information: Table S1)[38–42] with one molecule in the asymmetric unit.

The molecular structure confirmed the trigonal-pyramidal geometry around the silicon atom, with two N atoms from the amidinate ligand and the NH– group of the bulky aniline (Figure 1) occupying the three basal coordination sites and the lone pair of silicon atom in the apical position. The position of the hydrogen atom H1 attached to N1 was taken from the residual electron density map and refined freely. The angle between the centroid of the (CN_2Si) plane of the amidinate backbone and the Si–NH bond (102.5°) is considerably smaller than the same reported for R_2NSi(amidinate) (R=Cy 107.7° and ^{i}Pr 108.7°),[37] highlighting the stronger s character of the lone pair of the silicon atom in aminosilylene **1b**. This is further supported by the electronic occupancy of the 3s(Si) orbital, estimated from Natural Bonding Orbital (NBO) analysis for **1b**, Cy_2NSi(amidinate) and $^{i}Pr_2NSi$(amidinate) ($3s^{1.531}$, $3s^{1.424}$, and $3s^{1.428}$ respectively). The sum of the bond angles around the silicon atom (266.38°) is also consistent with the stereoactive lone pair at the silicon atom in **1b**. The Si–N bond lengths in **1b** are similar to those known for R_2NSi(amidinate) compounds.[37]

A reactive NH– group next to a naked Si(II) atom in **1a** and **1b** could facilitate a 1,2-hydrogen shift, forming silanimine with a π bond between Si and N atoms, as previously reported for 1,2-silyl shift with similar systems.[43–45] To check the 1,2-hydrogen shift to the Si(II) atom, a C_6D_6 solution of **1a** was heated at varying temperatures (50 °C, 70 °C and 80 °C), and the ^{1}H and ^{29}Si NMR spectra were recorded (see Supporting Information for details). No change was observed up to 50 °C; however, at 70 °C, almost 70% conversion to a new compound **2** was observed. Complete conversion occurred when the temperature was raised to 80 °C (Scheme 3). The ^{1}H NMR spectrum of the reaction mixture showed a new characteristic Si–H resonance at 6.15 ppm together with two distinct singlets at 5.60 and 3.91 ppm (see Supporting Information: Figure S23), each for one proton at Ph_2CH and NH–, respectively, suggesting the possible intramolecular C-



Scheme 3. Reactivity studies of **1a** and **1b** upon heating.

© 2023 The Authors. Angewandte Chemie International Edition published by Wiley-VCH GmbH

15213773, 2024, 9, Downloaded from https://onlinelibrary.wiley.com/doi/10.1002/anie.202317416, Wiley Online Library on [07/11/2026]. See the Terms and Conditions (https://onlinelibrary.wiley.com/terms-and-conditions) on Wiley Online Library for rules of use; OA articles are governed by the applicable Creative Commons License

(sp^3)–H activation of one of the methine hydrogen of side-arm benzhydryl groups to the Si(II) atom. Furthermore, the proton-coupled ^{29}Si NMR spectrum revealed a doublet of doublets centered at −46.96 ppm with a $^1J_{SiH}$ coupling of 274 Hz and a $^3J_{HH}$ coupling of 4.8 Hz, supporting the likely C(sp^3)–H activation (see Supporting Information: Figure S27). LIFDI mass spectrometry also confirmed the product formation with a $[M]^+$ ion at 697.3 (m/z = 697.3852). Additional evidence for the formation of **2** came from the IR spectra, which revealed N–H and Si–H stretching vibration at 3428 and 2105 cm^{-1}, respectively (see Supporting Information: Figure S29).

Single crystals of **2**, suitable for X-ray diffraction analysis, were obtained by growing them from a saturated hexane solution at room temperature (Figure 2). SC-XRD analysis confirmed the intramolecular C(sp^3)–H activation of the methine proton of the side-arm benzhydryl group, resulting in the formation of the rare cyclic silazane **2** featuring a five-membered heterocyclic ring instead of a 1,2-hydrogen shift. The positions of the hydrogen atoms H1 attached to Si1 and H2 bound to N1 were taken from the residual electron density map and refined freely. While silylene-assisted C(sp^3)–H activation is known with acyclic silylenes,[46–47] the C(sp^3)–H activation with base stabilized silylenes remains unexplored to the best of our knowledge. Notably, **1a** exhibits unusual reactivity and behaves as an acyclic silylene during the C(sp^3)–H activation reaction by opening the donor-stabilized dative bond of the amidinate.

The molecular structure showed two different types of ^{t}Bu groups. However, the ^{1}H NMR spectrum at room temperature showed only an averaged signal for both at 0.7 ppm. This is most likely due to facile Si–N bond rotation at room temperature. Variable-temperature ^{1}H NMR spectrum in THF-D_8 showed two well-resolved signals for 9 protons when the solution was cooled below −20 °C (see Supporting Information: Figure S24), indicating highly facile Si–N bond rotation at room temperature.

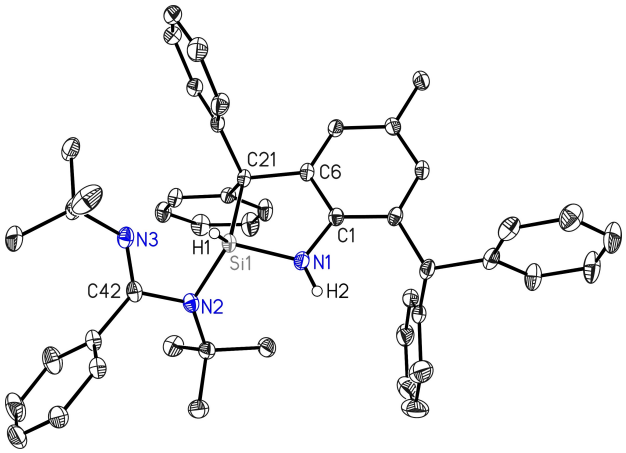


Figure 2. Molecular structure of **2**. The anisotropic displacement parameters are depicted at the 50% probability level. Hydrogen atoms, except NH, have been removed for clarity. Selected bond lengths (Å) and bond angles (°). Si1–N1 1.7503(11), Si1–N2 1.7644(11), Si1–C21 1.9441(12), C1–N1 1.3918(14), N1–Si1–N2 107.99(5), N1–Si1–C21 91.10(5), N2–Si1–C21 125.47(5).

However, in the case of **1b**, even after heating the solution at 80 °C, only 50 % conversion to **3** was achieved. Complete conversion was observed when the temperature was increased to 100 °C (Scheme 3). The ^{1}H NMR spectrum suggests a possible 1,2-hydrogen shift, with a new resonance for Si–H at 5.90 ppm, leading to rare silanimine **3** (see Supporting Information: Figure S30 and S34). This was further authenticated with the help of a doublet in the proton-coupled ^{29}Si NMR spectrum at −97.0 ppm with $^1J_{SiH}$ coupling of 275 Hz, and ^{29}Si{^{1}H} NMR spectrum showed only a singlet at −97.0 ppm (see Supporting Information: Figure S35). The LIFDI mass-spectrometry showed a molecular ion for $[M]^+$ at 519.9, whereas high-resolution mass spectrometry showed $[M+H]^+$ 520.4067 (m/z = 520.4082), confirming the rare silanimine **3** formation (see Supporting Information: Figures S36–S37). Additionally, the IR spectrum showed a stretching vibration at 2136 cm^{-1} for Si–H, further suggesting the formation of **3** (see Supporting Information: Figure S38). Unfortunately, even after several attempts, we could not get a single-crystal for the X-ray diffraction study. Nevertheless, the ^{1}H and ^{29}Si NMR spectra match those reported for similar systems.[48,45]

DFT calculations using Gaussian16[49] (B3LYP-D3/def2-SVP//B3LYP-D3/def2-TZVP, see Supporting Information for computational details) have been used to gain insight into the reaction mechanism for different reactivity patterns observed for the formations of **2** and **3** from **1a** and **1b**, respectively (Figure 3 and Table S9). The formation of **2** is an exergonic reaction ($\triangle G = -3.20$ kcal/mol) and involves intramolecular C(sp^3)–H activation of the benzhydryl group. The reaction mechanism proceeds via proton abstraction by Si(II) centre through $\mathbf{TS_{1a}}$**-1** (26.17 kcal/mol) and adds to the benzylic carbon of the side-arm benzhydryl group, leading to the formation of $\mathbf{Int_{1a}}$**-1**. This step is endergonic by 0.51 kcal/mol. A Si–N bond rearrangement in the second step leads to the final product **2** via $\mathbf{TS_{1a}}$**-2** (7.85 kcal/mol). The high energy barrier, i.e., $\mathbf{TS_{1a}}$**-1** at 26.17 kcal/mol, is concurrent with the elevated temperature and the longer time required for the intramolecular C–H insertion (80 °C and 24 h). It is worth mentioning that the 1,2-hydrogen shift in **1a** requires a higher energy barrier (51.69 kcal/mol, Figure S63), making it unfavourable. This contrasts with the 1,2-silyl shifts described by Scheschkewitz[50] and Nakata[45] in the formations of donor-stabilized silene and silanimine, respectively. Kira and co-workers also observed a similar 1,2-silyl shift in the isomerization of silylene to silene.[43] The energy of HOMO of Nakata's silylene (−4.34 eV) is higher than that of **1a** (−5.30 eV) and Kira's silylene (−5.48 eV) (see Supporting Information: Table S11 for details). This is consistent with a facile 1,2-silyl shift observed with Nakata's silylene to form silanimine. However, the facile 1,2-silyl migration with Kira's silylene might be due to smaller energy barrier for 1,2-silyl versus 1,2-hydrogen shifts in this class of compounds. Kira and Iwamoto have theoretically verified this in the silylene to silene conversion, where they found a relatively small barrier for the 1,2-silyl shift compared to the 1,2-hydrogen shift.[43]

© 2023 The Authors. Angewandte Chemie International Edition published by Wiley-VCH GmbH

15213773, 2024, 9, Downloaded from https://onlinelibrary.wiley.com/doi/10.1002/anie.202317416, Wiley Online Library on [07/11/2026]. See the Terms and Conditions (https://onlinelibrary.wiley.com/terms-and-conditions) on Wiley Online Library for rules of use; OA articles are governed by the applicable Creative Commons License

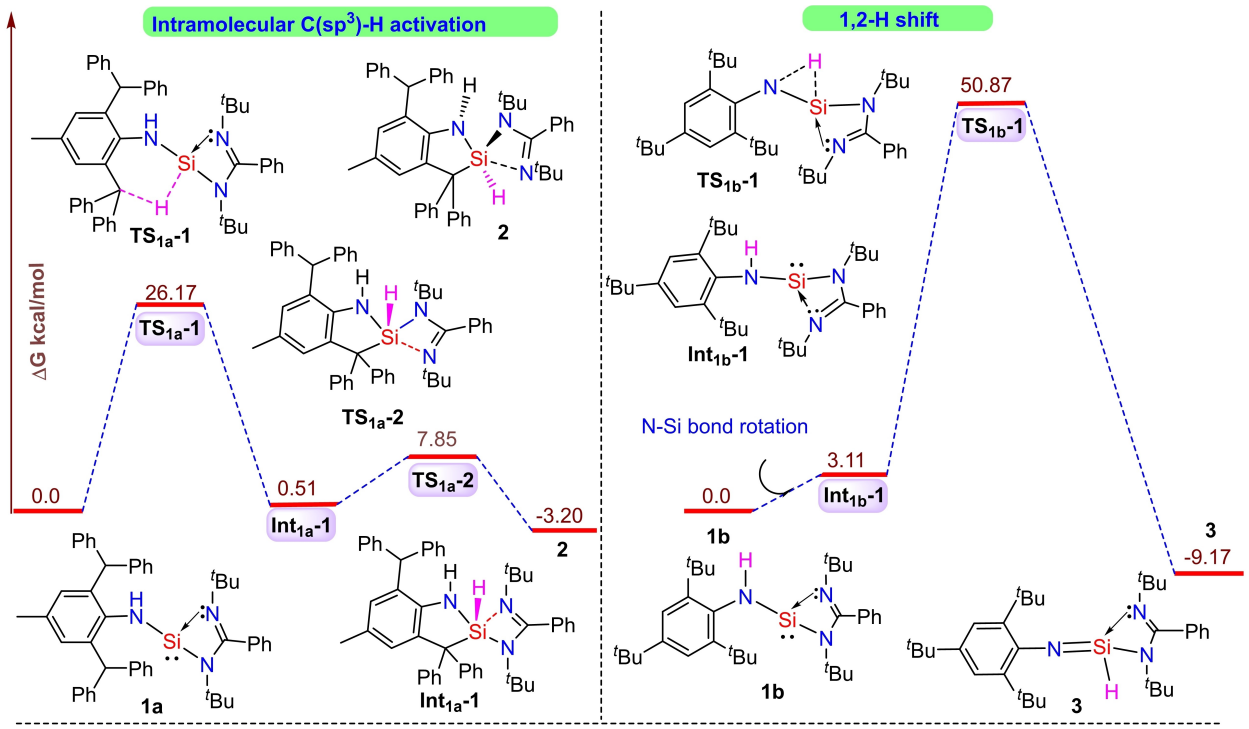
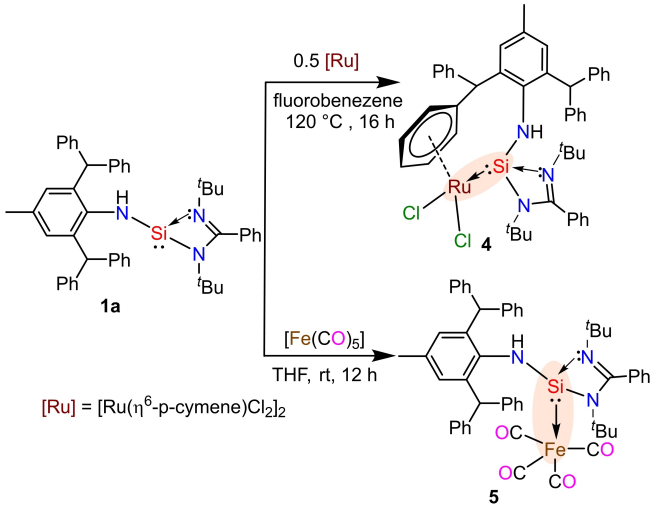


Figure 3. B3LYP-D3 computed energy profile diagram for intramolecular C(sp^3)–H activation in **1a** and 1,2-hydrogen shift in **1b**.

Unlike **1a**, complex **1b** shows a 1,2-hydrogen shift. This can be attributed to the absence of the analogous intramolecular (Ph_2C)H···Si interaction for **1b** and the thermodynamic equilibrium between **1b** and **3**, with the latter being favourable with the formation of Si=N (Figure 6h). Since the NH proton is oriented *trans* to the Si(II) lone pair, the first step involves the rotation of the Si–N bond to bring the NH proton and Si(II) lone pair in close proximity in the same plane. This step is endergonic by 3.11 kcal/mol (**Int_{1b}-1**, Figure 3). Next, the 1,2-hydrogen shift occurs via a **TS_{1b}-1** (50.87 kcal/mol) to give **3**. This is further supported by the fact that very harsh conditions and prolonged heating (100 °C and four days) were required to generate **3**. A similar higher energy barrier for the reverse reaction, a 1,2-hydrogen shift from silanimine to aminosilylene, was reported earlier.[51] To the best of our knowledge, this is the first report on experimental verification of 1,2-hydrogen shift in silylenes. The 1,2-hydrogen shift to **3** was very sensitive to reaction conditions; even a slight decrease in temperature and reaction time affected the product yield considerably (Figure S39). The product was only obtained when the reaction was carried in a thin glass screw-capped NMR tube.

In order to explore the potential of free aminosilylene, **1a**, as a ligand and its stability and ligating capabilities, it was treated with Ru(II) and Fe(0) precursors. The aminosilylene **1a** with bulky benzhydryl pendant arms might form rare, tethered complexes involving phenyl groups as (η^2-η^6) donors. The reaction of **1a** with [Ru(η^6-*p*-cymene)Cl_2]$_2$ in 2:1 ratios in fluorobenzene at 120 °C resulted in tethered complex **4** as confirmed by spectroscopic and structural studies. Phosphine and nitrogen donor ligands have all been shown to generate tethered Ru complexes under suitable conditions.[52–53] However, silylene ligands are not prevalent in such complexes.[54]

Further, treatment of **1a** with [$Fe(CO)_5$] resulted in the formation of Fe(0) complex **5** as a red solid in good yield (Scheme 4). Driess and co-workers have studied the reactivity of Ni-protected N-heterocyclic silylene (NHSi) with RNH_2 to generate the aminosilylene in the coordination sphere of Ni(0).[14,15] In contrast, our work stems from free



Scheme 4. Synthesis of Ru(II) and Fe(0) complexes **4** and **5**.

© 2023 The Authors. Angewandte Chemie International Edition published by Wiley-VCH GmbH

15213773, 2024, 9, Downloaded from https://onlinelibrary.wiley.com/doi/10.1002/anie.202317416, Wiley Online Library on [07/11/2026]. See the Terms and Conditions (https://onlinelibrary.wiley.com/terms-and-conditions) on Wiley Online Library for rules of use; OA articles are governed by the applicable Creative Commons License

aminosilylene **1a** to afford Ru(II) and Fe(0) complexes. Both complexes were thoroughly characterized by various spectroscopic techniques. The ^{1}H NMR spectrum of **4** suggested the η^6-coordinated rare tethered complex formation with characteristic resonances: multiplet at δ 5.69, a broad singlet at 5.99, and doublets with a coupling of 5.7 Hz at 4.92 and 4.79 ppm. The ^{29}Si{^{1}H} NMR spectra of **4** and **5** showed singlets at 31.6 and 55.6 ppm, respectively, with a coordination shift of 34.9 and 59 ppm compared to free aminosilylene **1a**. The ^{29}Si{^{1}H} NMR spectrum of **4** showed a significantly upfield chemical shift compared to that of **5**, indicating increased electron density on the silicon atom in **4**. The ^{13}C{^{1}H} NMR spectrum of **4** also showed characteristic resonances at δ 72.40, 78.45, 97.79, 98.89, and 100.49 ppm, suggesting the η^6-arene coordination of one of the side arms benzhydryl group. Whereas the ^{13}C{^{1}H} NMR spectrum of **5** showed singlet at 216.67 ppm for the carbonyl group, which is similar to the same in the base stabilized Fe(0) complex of silylene.[55] The LIFDI mass spectra of **4** and **5** showed the molecular ions $(M)^+$ at 869.1 (m/z = 869.2273) and 865.2 (m/z = 865.2998), confirming the complexes formation. Single-crystal X-ray diffraction studies unambiguously established the molecular structures **4** and **5**. The red-block-shaped crystals of **4** were obtained from the saturated solution of fluorobenzene. In contrast, the yellow needles of **5** were obtained from a saturated diethyl ether solution at room temperature over a period of 2 days.

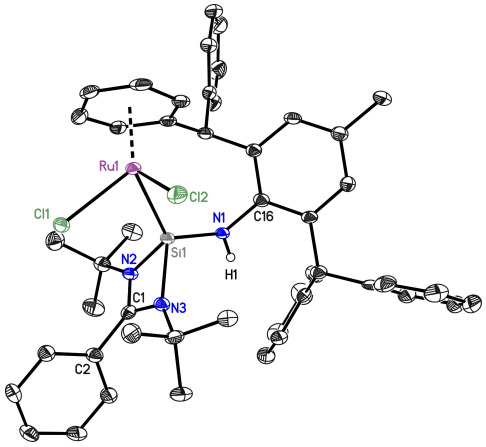


Figure 4. Molecular structure of **4**. The anisotropic displacement parameters are depicted at the 50% probability level. Hydrogen atoms except NH– have been omitted for the sake of clarity. Selected bond lengths (Å) and bond angles (°): N1–Si1 1.724(3), N2–Si1 1.846(3), N3–Si1 1.872(3), Ru1–Si1 2.3409(10), Ru1–Cl1 2.4209(9), Ru1–Cl2 2.4117(10), Ru1–C from 2.176(3) (C9) to 2.302(4) (C12); N1–Si1–N2 104.24(15), N1–Si1–N3 108.05(14), Si1–Ru1–Cl1 84.90(3), Si1–Ru1–Cl2 88.63(3), Cl1–Ru1–Cl2 89.96(4).

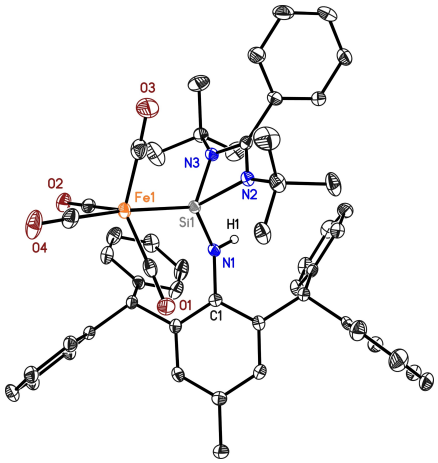


Figure 5. Molecular structure of **5**. The anisotropic displacement parameters are depicted at the 50% probability level. Hydrogen atoms except NH– have been omitted for the sake of clarity. Selected bond lengths (Å) and bond angles (°): N1–Si1 1.7203(14), N2–Si1 1.8708 (14), N3–Si1 1.8171(14), Fe1–Si1 2.2545(6), Fe1–C49 1.7698(18), Fe1–C50 1.781(2), Fe1–C51 1.7763(18), Fe1–C52 1.7871(19). N1–Si1–N2 109.45(6), N1–Si1–N3 102.10(7), N1–Si1–Fe1 124.60(5), Si1–Fe1–C49 81.02(5), Si1–Fe1–C50 85.51(6), Si1–Fe1–C51 95.35(5), Si1–Fe1–C52 171.36(6).

The positions of the hydrogen atoms H1 attached to N1 in both structures were taken from the residual electron density map and refined freely. Figures 4 and 5 depict both views of the molecular structures of **4** and **5**. The crystallographic data and the details of the structure determination are given in ESI,[38–42] and the selected bond lengths (Å) and the bond angles (°) are given in the Figure captions.[56] Complexes **4** and **5** crystallized in monoclinic crystal systems with $P2_1/n$ and $P2_1/c$ space groups, respectively (see Supporting Information: Table S2–6). In the asymmetric unit of **4**, one molecule is present with three molecules of fluorobenzene as a lattice solvent of crystallization. The molecular structure of **4** confirms the formation of the rare η^6-arene tethered complex formation. The Ru complex **4** adopts the three-legged "*piano stool*" geometry. The Ru1–Si1 bond length of 2.3409(10) Å is slightly longer than the same in Ru(II) complexes of silylene-based ligands.[57–58] The Ru–Cl bond lengths are unexceptional and fall within the range of previously reported similar complexes.[57,53]

In the asymmetric unit of **5**, only one molecule is present. The molecular structure of **5** shows the trigonal-bipyramidal arrangement around the Fe atom with bulky aminosilylene ligand **1a** occupying one of the apical positions to minimize the steric repulsion and four CO groups occupying the other four sites. The apical position of **1a** in complex **5** is akin to other strcutrally similar Fe(0) complexes of bulky silylene ligands [(PhC(N^{t}Bu)$_2$)-(O^{t}Bu)Si:→Fe(CO)$_4$][55] and [{Me$_2$NC(N^{t}Bu)(NDipp)}-(H)Si:→Fe(CO)$_4$].[59] The Fe1–Si1 bond length in complex **5** (2.2545(6) Å) is slightly longer than the same observed in similar complexes, [(PhC(N^{t}Bu)$_2$)(O^{t}Bu)Si:→Fe(CO)$_4$] (2.237(7) Å)[55] and [{Me$_2$NC(N^{t}Bu)(NDipp)}(H)Si:→Fe-(CO)$_4$] (2.234(1) Å)[59] and are similar to [Fe(CO)$_4$\{NMe$_2$Si-(PhC(NDipp)$_2$)\}][60] (2.2574(7) Å).[60] The average Fe–C_{CO} bond length of 1.778 Å in **5** is in the range observed in similar complexes such as [(PhC(N^{t}Bu)$_2$)(O^{t}Bu)Si:→Fe-(CO)$_4$] (1.769 Å),[55] and [{Me$_2$NC(N^{t}Bu)(NDipp)}(H)Si:→Fe(CO)$_4$] (1.779 Å).[59] The Fe–C_{CO} bonds *trans* to the Si(II) atom (Fe(1)–C(52) = 1.7871(19) Å) in complex **5** are slightly longer than the same found in the equatorial positions. This

© 2023 The Authors. Angewandte Chemie International Edition published by Wiley-VCH GmbH

15213773, 2024, 9, Downloaded from https://onlinelibrary.wiley.com/doi/10.1002/anie.202317416, Wiley Online Library on [07/11/2026]. See the Terms and Conditions (https://onlinelibrary.wiley.com/terms-and-conditions) on Wiley Online Library for rules of use; OA articles are governed by the applicable Creative Commons License

can be attributed to the better σ-donor ability of the Si(II) atom in complex **5**.

We have further conducted DFT analyses on **1**–**5** using Gaussian16[49] to elucidate the structural, bonding and energetic aspects. The optimized structures for **1b**, **2**, **4**, and **5** (using B3LYP-D3 functional,[61–64] LANL2TZ basis set[65–66] for Ru, Fe; TZVP basis set for Si, Cl; and SVP basis set for O, N, C and H atoms) are in excellent agreement with the XRD structures (Figure S50–54 and Table S7).[67–68] This gives confidence in the optimized structures for **1a** and **3** (Figure S54 and Table S7). Interestingly, the single point calculations (B3LYPD3/def2-TZVP)[69] on the optimized structures for **1**–**5** suggest that for **1**–**3**, the highest occupied molecular orbital (HOMO) is a π-type orbital centred on the substituted-amino group and Si atom. In contrast, the lowest unoccupied molecular orbital (LUMO) is π*-type, centred on the aromatic ring of the silylene group (Figure S55). It is worth mentioning here that the HOMO for **1a** has a prominent contribution from the 3s orbital of Si (Figure 6a and S55), advocating its reactivity toward $[Ru(\eta^6\text{-}p\text{-cymene})Cl_2]_2$ and $[Fe(CO)_5]$, leading to the formation of **4** and **5**. For **4**, the HOMO is centred on $\{RuCl_2\}$ group where the $Ru(d_{xy})$ orbital has π* type interaction with both $Cl(3p_y)$ ions. However, the LUMO is centred on the $\{RuCl_2Ph\}$

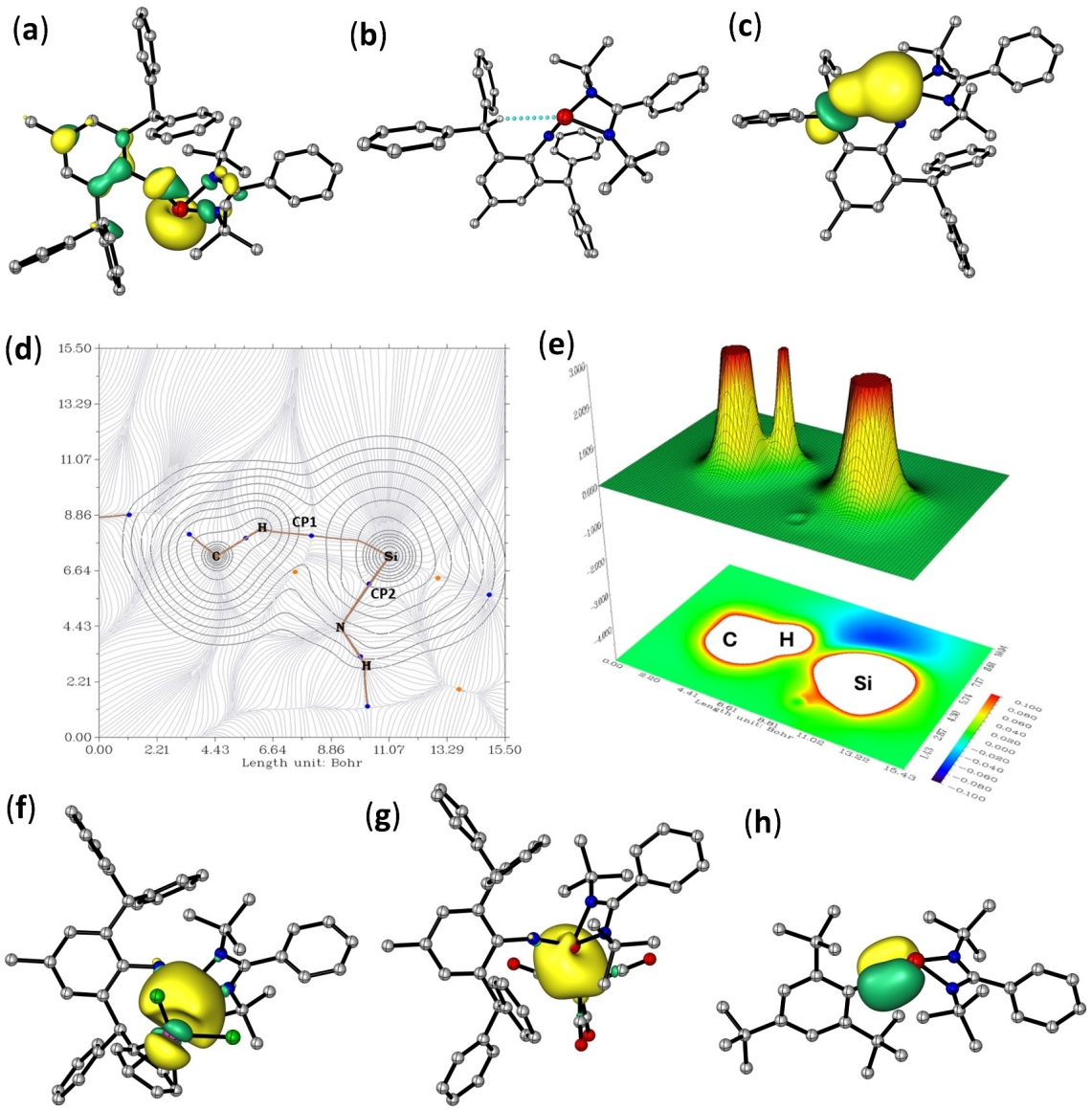


Figure 6. (a) DFT computed HOMO for **1a** centred on the substituted-amino group and Si atom; (b) DFT optimised molecular structure of **1a** showing intramolecular $(Ph_2C)H\cdots Si$ interaction along with the (c) NBO computed donor-acceptor plot for the same $\{[Si(3s^{0.60}3p_x^{0.40})\rightarrow \{C(2s2p_{x/y/z})^{0.37}-H(1s^{0.63})\}]=8.0$ kcal/mol}. (d) DFT-QTAIM computed contour map for **1a** showing intramolecular $(Ph_2C)H\cdots Si$ interaction (CP1) and (e) total electrostatic potential (ESP) map for **1a** showing electron localization between $(Ph_2C)H\cdots Si$. NBO based bonding orbitals for (f) **4** depicting strong Si–Ru interaction $\{Ru(5s^{0.28}5p_y^{0.22}4d_{xz/yz/x2-y2}^{0.50})^{0.58}-Si(3s^{0.66}3p_y^{0.33})^{0.42}\}$ with electronic occupation 1.865; (g) **5** showing strong Si–Fe interactions $\{Fe(5s^{0.24}4p_{x/y/z}^{0.53}3d_{xz/yz/xy}^{0.23})^{0.57}-Si(3s^{0.60}3p_x^{0.38})^{0.43}\}$ with electronic occupation 1.604; and (h) **3** showing strong Si=N bonding $\{Si(3p_z)^{0.13}-N(2p_z)^{0.87}\}$ with electronic occupation 1.800.

© 2023 The Authors. Angewandte Chemie International Edition published by Wiley-VCH GmbH

15213773, 2024, 9, Downloaded from https://onlinelibrary.wiley.com/doi/10.1002/anie.202317416, Wiley Online Library on [07/11/2026]. See the Terms and Conditions (https://onlinelibrary.wiley.com/terms-and-conditions) on Wiley Online Library for rules of use; OA articles are governed by the applicable Creative Commons License

group with Ru($d_{x^2-y^2}$) interacting with Ph(π) and Cl($3p_s$) orbitals (Figure S55). For **5**, the HOMO is {Fe(CO)$_4$} centred where Fe($d_{x^2-y^2}$) interacts with CO(π^*) orbitals. In comparison, the LUMO is π^*-type, centred on the substituted silylene group (Figure S55). For **1a** and **2**, the calculated HOMO–LUMO energy gap is found to be more than **1b** [$\Delta E_{HOMO\text{-}LUMO}$ in *ev*; **2**(4.18) ≥ **1a**(4.14) > **1b**(3.87)]. This can be attributed to the higher stabilization of HOMO for **1a** and **2** due to the four Ph- groups. Second-order perturbation theory analysis of fock matrix in natural bonding orbital (NBO) basis[70–71] and Quantum Theory of Atoms in Molecule (QTAIM)[72–73] suggest strong intramolecular (Ph_2C)H···Si interaction for **1a** ([Si($3s^{0.60}3p_x^{0.40}$)→{C($2s2p_{x/y/z}$)$^{0.37}$–H($1s^{0.63}$)}] = 8.0 kcal mol^{-1}; and electron density of $\rho = 0.027$ e Bohr^{-3}), favouring thermodynamic equilibrium between **1a** and **2** with later being favourable, thus reasoning the intramolecular C(sp^3)–H activation for **1a** with the weakening of Si–N bond (Figure 6b–e, S56 and Table S8). NBO and DFT-QTAIM analysis in **4** suggest strong Si($3s3p_{x/y}$)→Ru($5s5p_{x/y/z}4d_{xz}$) electron transfer. Whereas in **5**, due to filled valence orbitals (4s/4p/3d), Si→Fe electron transfer is not observed (Figure 6f–g, S56–62 and Table S8). It is worth mentioning here that both in **4** and **5**, Ru/Fe→Si electron transfer is observed.

Conclusion

In summary, we have successfully reported the synthesis of so far elusive aminosilylenes **1a** and **1b** containing an NH– unit next to the naked Si(II) atom. The bulky groups in the ligand periphery might be the key to the stabilization. The aminosilylene **1a** on heating, showed unique reactivity by activating C(sp^3)–H bond of the benzhydryl side-arms to afford silazane **2**, featuring NH–SiH direct linkage. However, with **1b**, a 1,2-hydrogen shift afforded a rare silanimine **3** with a hydrido ligand attached to the unsaturated silicon atom. To the best of our knowledge, this work represents the first example of the experimental and theoretical verification of 1,2-hydrogen shift in aminosilylene to silanimine conversion. The coordination capabilities of **1a** were also explored in Ru(II) and Fe(0) complexation. The aminosilylene **1a** forms the mononuclear (κ^1-*Si*) complex with [Fe(CO)$_5$]. In contrast, with [Ru(η^6-*p*-cymene)Cl$_2$]$_2$, a κ^1-*Si*-η^6-arene complex is formed where Si acts as two electron σ-donor atom and a benzhydryl arene acts as a 6e$^-$ η^6 π donor. Hence, the aminosilylene **1a** acts as an 8e$^-$ donor in **4**. The aminosilylene reported in this work is an analogue of well-studied aminophosphine ($RNHPR_2$). We hope our work opens a new arena in silylene chemistry where this class of compounds can be used as a non-innocent ligand in bond-making and breaking processes.

Supporting Information

The data that support the findings of this study are available in the Supporting Information of this article. The additional references within the Supporting Information.[74–76]

Acknowledgements

D. S. and K. R. thank the GRK BENCh, which is funded by the Deutsche Forschungsgemeinschaft, German Research Foundation (grant No. 389479699/GRK2455). MKS thanks Edinburgh Compute and Data Facility (ECDF) (http://www.ecdf.ed.ac.uk/) for computing resources. Open Access funding enabled and organized by Projekt DEAL.

Conflict of Interest

The authors declare no conflict of interest.

Data Availability Statement

The data that support the findings of this study are available in the supplementary material of this article.

Keywords: 1,2-Hydrogen Shift · Aminophosphine · Aminosilylene · Protic N-Heterocyclic Carbene · Silylene

[1] S. K. Mandal, H. W. Roesky, *Acc. Chem. Res.* **2012**, *45*, 298–307.
[2] R. S. Ghadwal, R. Azhakar, H. W. Roesky, *Acc. Chem. Res.* **2013**, *46*, 444–456.
[3] G. Frenking, R. Tonner, S. Klein, N. Takagi, T. Shimizu, A. Krapp, K. K. Pandey, P. Parameswaran, *Chem. Soc. Rev.* **2014**, *43*, 5106–5139.
[4] S. Yao, Y. Xiong, M. Driess, *Acc. Chem. Res.* **2017**, *50*, 2026–2037.
[5] T. J. Hadlington, M. Driess, C. Jones, *Chem. Soc. Rev.* **2018**, *47*, 4176–4197.
[6] C. Mohapatra, H. Darmandeh, H. Steinert, B. Mallick, K.-S. Feichtner, V. H. Gessner, *Chem. Eur. J.* **2020**, *26*, 15145–15149.
[7] S. Yao, Y. Xiong, A. Saddington, M. Driess, *Chem. Commun.* **2021**, *57*, 10139–10153.
[8] R. S. Simons, L. Pu, M. M. Olmstead, P. P. Power, *Organometallics* **1997**, *16*, 1920–1925.
[9] A. D. Phillips, R. J. Wright, M. M. Olmstead, P. P. Power, *J. Am. Chem. Soc.* **2002**, *124*, 5930–5931.
[10] P. P. Power, *Chem. Rev.* **2003**, *103*, 789–810.
[11] G. H. Spikes, J. C. Fettinger, P. P. Power, *J. Am. Chem. Soc.* **2005**, *127*, 12232–12233.
[12] P. P. Power, *Organometallics* **2007**, *26*, 4362–4372.
[13] H. F. Schaefer III, *Acc. Chem. Res.* **1979**, *12*, 288–296.
[14] A. Meltzer, C. Präsang, M. Driess, *J. Am. Chem. Soc.* **2009**, *131*, 7232–7233.
[15] A. Meltzer, S. Inoue, C. Präsang, M. Driess, *J. Am. Chem. Soc.* **2010**, *132*, 3038–3046.
[16] R. Yadav, X. Sun, R. Köppe, M. T. Gamer, F. Weigend, P. W. Roesky, *Angew. Chem. Int. Ed.* **2022**, *61*, e202211115.
[17] M. C. Jahnke, F. E. Hahn, *Coord. Chem. Rev.* **2015**, *293–294*, 95–115.
[18] S. Kuwata, F. E. Hahn, *Chem. Rev.* **2018**, *118*, 9642–9677.
[19] L. J. L. Häller, S. A. Macgregor, *Eur. J. Inorg. Chem.* **2009**, 2000–2006.
[20] Z. Yang, C. He, S. Goettl, R. I. Kaiser, V. N. Azyazov, A. M. Mebel, *J. Am. Chem. Soc.* **2021**, *143*, 14227–14234.

© 2023 The Authors. Angewandte Chemie International Edition published by Wiley-VCH GmbH

15213773, 2024, 9, Downloaded from https://onlinelibrary.wiley.com/doi/10.1002/anie.202317416, Wiley Online Library on [07/11/2026]. See the Terms and Conditions (https://onlinelibrary.wiley.com/terms-and-conditions) on Wiley Online Library for rules of use; OA articles are governed by the applicable Creative Commons License

[21] M. Denk, R. Lennon, R. Hayashi, R. West, A. V. Belyakov, H. P. Verne, A. Haaland, M. Wagner, N. Metzler, *J. Am. Chem. Soc.* **1994**, *116*, 2691–2692.
[22] M. Haaf, T. A. Schmedake, R. West, *Acc. Chem. Res.* **2000**, *33*, 704–714.
[23] L. Wang, Y. Li, Z. Li, M. Kira, *Coord. Chem. Rev.* **2022**, *457*, 214413.
[24] C.-W. So, H. W. Roesky, J. Magull, R. B. Oswald, *Angew. Chem. Int. Ed.* **2006**, *45*, 3948–3950.
[25] D. Stalke, M. Wedler, F. T. Edelmann, *J. Organomet. Chem.* **1992**, *431*, C1–C5.
[26] S. S. Sen, H. W. Roesky, D. Stern, J. Henn, D. Stalke, *J. Am. Chem. Soc.* **2010**, *132*, 1123–1126.
[27] B. Blom, M. Stoelzel, M. Driess, *Chem. Eur. J.* **2013**, *19*, 40–62.
[28] S. K. Kushvaha, P. Kallenbach, S. M. N. V. T. Gorantla, R. Herbst-Irmer, D. Stalke, H. W. Roesky, *Chem. Eur. J.* **2023**, e202303113.
[29] Z. Benedek, T. Szilvási, *RSC Adv.* **2015**, *5*, 5077–5086.
[30] Y. Wang, M. Karni, S. Yao, Y. Apeloig, M. Driess, *J. Am. Chem. Soc.* **2019**, *141*, 1655–1664.
[31] S. Yao, A. Kostenko, Y. Xiong, A. Ruzicka, M. Driess, *J. Am. Chem. Soc.* **2020**, *142*, 12608–12612.
[32] S. Yao, A. Saddington, Y. Xiong, M. Driess, *Acc. Chem. Res.* **2023**, *56*, 475–488.
[33] B. Blom, D. Gallego, M. Driess, *Inorg. Chem. Front.* **2014**, *1*, 134–148.
[34] T. J. Hadlington, T. Szilvási, M. Driess, *J. Am. Chem. Soc.* **2019**, *141*, 3304–3314.
[35] K. Hansen, T. Szilvási, B. Blom, M. Driess, *J. Am. Chem. Soc.* **2014**, *136*, 14207–14214.
[36] J. R. Khusnutdinova, D. Milstein, *Angew. Chem. Int. Ed.* **2015**, *54*, 12236–12273.
[37] R. Azhakar, R. S. Ghadwal, H. W. Roesky, H. Wolf, D. Stalke, *Organometallics* **2012**, *31*, 4588–4592.
[38] S. v. A. Bruker AXS Inc., Madison, **2016**.
[39] C. B. Hübschle, G. M. Sheldrick, B. Dittrich, *J. Appl. Crystallogr.* **2011**, *44*, 1281–1284.
[40] L. Krause, R. Herbst-Irmer, G. M. Sheldrick, D. Stalke, *J. Appl. Crystallogr.* **2015**, *48*, 3–10.
[41] G. Sheldrick, *Acta Crystallogr. Sect. C* **2015**, *71*, 3–8.
[42] G. Sheldrick, *Acta Crystallogr. Sect. A* **2015**, *71*, 3–8.
[43] S. Ishida, T. Iwamoto, M. Kira, *Organometallics* **2009**, *28*, 919–921.
[44] S. Inoue, W. Wang, C. Präsang, M. Asay, E. Irran, M. Driess, *J. Am. Chem. Soc.* **2011**, *133*, 2868–2871.
[45] S. Takahashi, A. Ishii, N. Nakata, *Chem. Commun.* **2021**, *57*, 3203–3206.
[46] A. V. Protchenko, K. H. Birjkumar, D. Dange, A. D. Schwarz, D. Vidovic, C. Jones, N. Kaltsoyannis, P. Mountford, S. Aldridge, *J. Am. Chem. Soc.* **2012**, *134*, 6500–6503.
[47] A. V. Protchenko, A. D. Schwarz, M. P. Blake, C. Jones, N. Kaltsoyannis, P. Mountford, S. Aldridge, *Angew. Chem. Int. Ed.* **2013**, *52*, 568–571.
[48] H. Cui, C. Cui, *Chem. Asian J.* **2011**, *6*, 1138–1141.
[49] Gaussian 16, Revision C.01, M. J. Frisch, G. W. Trucks, H. B. Schlegel, G. E. Scuseria, M. A. Robb, J. R. Cheeseman, G. Scalmani, V. Barone, G. A. Petersson, H. Nakatsuji, X. Li, M. Caricato, A. V. Marenich, J. Bloino, B. G. Janesko, R. Gomperts, B. Mennucci, H. P. Hratchian, J. V. Ortiz, A. F. Izmaylov, J. L. Sonnenberg, Williams, F. Ding, F. Lipparini, F. Egidi, J. Goings, B. Peng, A. Petrone, T. Henderson, D. Ranasinghe, V. G. Zakrzewski, J. Gao, N. Rega, G. Zheng, W. Liang, M. Hada, M. Ehara, K. Toyota, R. Fukuda, J. Hasegawa, M. Ishida, T. Nakajima, Y. Honda, O. Kitao, H. Nakai, T. Vreven, K. Throssell, J. A. Montgomery, Jr., J. E. Peralta, F. Ogliaro, M. J. Bearpark, J. J. Heyd, E. N. Brothers, K. N. Kudin, V. N. Staroverov, T. A. Keith, R. Kobayashi, J. Normand, K. Raghavachari, A. P. Rendell, J. C. Burant, S. S. Iyengar, J. Tomasi, M. Cossi, J. M. Millam, M. Klene, C. Adamo, R. Cammi, J. W. Ochterski, R. L. Martin, K. Morokuma, O. Farkas, J. B. Foresman, D. J. Fox, Wallingford, CT, **2016**.
[50] T. Imagawa, L. Giarrana, D. M. Andrada, B. Morgenstern, M. Nakamoto, D. Scheschkewitz, *J. Am. Chem. Soc.* **2023**, *145*, 4757–4764.
[51] T. N. Truong, M. S. Gordon, *J. Am. Chem. Soc.* **1986**, *108*, 1775–1778.
[52] H. G. Nedden, A. Zanotti-Gerosa, M. Wills, *Chem. Rec.* **2016**, *16*, 2623–2643.
[53] M. K. Pandey, J. T. Mague, M. S. Balakrishna, *Inorg. Chem.* **2018**, *57*, 7468–7480.
[54] Y. Bai, J. Zhang, C. Cui, *Chem. Commun.* **2018**, *54*, 8124–8127.
[55] W. Yang, H. Fu, H. Wang, M. Chen, Y. Ding, H. W. Roesky, A. Jana, *Inorg. Chem.* **2009**, *48*, 5058–5060.
[56] Deposition numbers 2300361 (for **1b**), 2300362 (for **2**), 2266917 (for **4**), and 2266918 (for **5**) contain the supplementary crystallographic data for this paper. These data are provided free of charge by the joint Cambridge Crystallographic Data Centre and Fachinformationszentrum Karlsruhe Access Structures service.
[57] H. Yoo, P. J. Carroll, D. H. Berry, *J. Am. Chem. Soc.* **2006**, *128*, 6038–6039.
[58] H. Hashimoto, J. Sato, H. Tobita, *Organometallics* **2009**, *28*, 3963–3965.
[59] B. Blom, M. Pohl, G. Tan, D. Gallego, M. Driess, *Organometallics* **2014**, *33*, 5272–5282.
[60] R. Tacke, C. Kobelt, J. A. Baus, R. Bertermann, C. Burschka, *Dalton Trans.* **2015**, *44*, 14959–14974.
[61] A. D. Becke, *Phys. Rev. A* **1988**, *38*, 3098–3100.
[62] C. Lee, W. Yang, R. G. Parr, *Phys. Rev. B* **1988**, *37*, 785–789.
[63] A. D. Becke, *J. Chem. Phys.* **1993**, *98*, 5648–5652.
[64] S. Grimme, J. Antony, S. Ehrlich, H. Krieg, *J. Chem. Phys.* **2010**, *132*, 154104.
[65] L. E. Roy, P. J. Hay, R. L. Martin, *J. Chem. Theory Comput.* **2008**, *4*, 1029–1031.
[66] B. P. Pritchard, D. Altarawy, B. Didier, T. D. Gibson, T. L. Windus, *J. Chem. Inf. Model.* **2019**, *59*, 4814–4820.
[67] A. Schäfer, H. Horn, R. Ahlrichs, *J. Chem. Phys.* **1992**, *97*, 2571–2577.
[68] A. Schäfer, C. Huber, R. Ahlrichs, *J. Chem. Phys.* **1994**, *100*, 5829–5835.
[69] F. Weigend, R. Ahlrichs, *Phys. Chem. Chem. Phys.* **2005**, *7*, 3297–3305.
[70] J. P. Foster, F. Weinhold, *J. Am. Chem. Soc.* **1980**, *102*, 7211–7218.
[71] M. K. Singh, N. Yadav, G. Rajaraman, *Chem. Commun.* **2015**, *51*, 17732–17735.
[72] H. L. Schmider, A. D. Becke, *J. Mol. Struc-THEOCHEM* **2000**, *527*, 51–61.
[73] T. Lu, F. Chen, *J. Comput. Chem.* **2012**, *33*, 580–592.
[74] F. Weigend, *Phys. Chem. Chem. Phys.* **2006**, *8*, 1057–1065.
[75] A. V. Marenich, C. J. Cramer, D. G. Truhlar, *J. Phys. Chem. B* **2009**, *113*, 6378–6396.
[76] G. Berthon-Gelloz, M. A. Siegler, A. L. Spek, B. Tinant, J. N. H. Reek, I. E. Markó, *Dalton Trans.* **2010**, *39*, 1444–1446.

Manuscript received: November 16, 2023
Accepted manuscript online: December 22, 2023
Version of record online: January 19, 2024

© 2023 The Authors. Angewandte Chemie International Edition published by Wiley-VCH GmbH

15213773, 2024, 9, Downloaded from https://onlinelibrary.wiley.com/doi/10.1002/anie.202317416, Wiley Online Library on [07/11/2026]. See the Terms and Conditions (https://onlinelibrary.wiley.com/terms-and-conditions) on Wiley Online Library for rules of use; OA articles are governed by the applicable Creative Commons License